LETTERS

GABA regulates synaptic integration of newly generated neurons in the adult brain

Shaoyu Ge[1]*, Eyleen L. K. Goh[1]*, Kurt A. Sailor[1], Yasuji Kitabatake[1], Guo-li Ming[1] & Hongjun Song[1]

Adult neurogenesis, the birth and integration of new neurons from adult neural stem cells, is a striking form of structural plasticity and highlights the regenerative capacity of the adult mammalian brain[1–8]. Accumulating evidence suggests that neuronal activity regulates adult neurogenesis and that new neurons contribute to specific brain functions[1–8]. The mechanism that regulates the integration of newly generated neurons into the pre-existing functional circuitry in the adult brain is unknown. Here we show that newborn granule cells in the dentate gyrus of the adult hippocampus are tonically activated by ambient GABA (γ-aminobutyric acid) before being sequentially innervated by GABA- and glutamate-mediated synaptic inputs. GABA, the major inhibitory neurotransmitter in the adult brain, initially exerts an excitatory action on newborn neurons owing to their high cytoplasmic chloride ion content[9–12]. Conversion of GABA-induced depolarization (excitation) into hyperpolarization (inhibition) in newborn neurons leads to marked defects in their synapse formation and dendritic development *in vivo*. Our study identifies an essential role for GABA in the synaptic integration of newly generated neurons in the adult brain, and suggests an unexpected mechanism for activity-dependent regulation of adult neurogenesis, in which newborn neurons may sense neuronal network activity through tonic and phasic GABA activation.

Using a retroviral strategy to express green fluorescent protein (GFP) specifically in proliferating cells and their progeny[6,7], we examined the synaptic integration of newly generated granule cells (DGCs) in the dentate gyrus of adult mice (Fig. 1). Retroviral labelling provides adequate time resolution for birth-dating and does not seem to affect the neuronal development of labelled cells (Fig. 1a, Supplementary Fig. 1, Supplementary Videos 1, 2 and Supplementary Table 1). To monitor the integration of new neurons in the adult brain, we used whole-cell patch clamping and recorded from GFP^+ DGCs in slices prepared from virus-infected animals (see Methods). Three days post viral injection (3 dpi), none of the GFP^+ cells recorded under voltage-clamp ($V_m = -65$ mV) showed any spontaneous synaptic currents (SSCs) or any detectable evoked postsynaptic currents (PSCs) when the perforant pathway was stimulated ($n = 15$; Fig. 1b–d). However, bath application of bicuculline (100 μM), a specific $GABA_A$ receptor antagonist[13,14], revealed the presence of a tonic current in all GFP^+ DGCs recorded from 3 dpi and onwards ($n = 48$; Fig. 1b). SR95531 (100 μM), another $GABA_AR$ antagonist[13,14], also abolished the tonic current (Supplementary Fig. 2a). In contrast, NO-711 (2.5 μM), a specific GABA transporter inhibitor[13,14], significantly enhanced the tonic current (Supplementary Fig. 2b). Notably, stimulation of local interneurons, such as basket cells[15], also enhanced the tonic currents in newborn DGCs (Supplementary Fig. 2c). Thus, newborn DGCs in the adult brain are tonically activated by ambient GABA before any detectable phasic/synaptic activation. Bicuculline (10 μM)-sensitive GABA-mediated PSCs (Fig. 1c) and CNQX (50 μM)-sensitive glutamate-mediated PSCs (Fig. 1d) were first detected in some GFP^+ DGCs at 7 dpi and 14 dpi, respectively. These results show that newborn neurons in the adult brain, as in neonates, follow a stereotypical integration process—first receiving tonic GABA activation, then GABA-mediated synaptic inputs and finally glutamate-mediated synaptic inputs[9,10,16–20].

To determine the nature of GABA activation, we made perforated whole-cell patch-clamp recordings using gramicidin (25 μg ml^{-1}) to allow reliable recording of GABA-induced currents[21]. We found that the reversal potential for GABA-induced currents (E_{GABA}) in GFP^+ DGCs gradually decreased during maturation (Fig. 2a, Supplementary Fig. 3a), indicating a higher concentration of intracellular chloride $[Cl^-]_i$ in younger neurons (Supplementary Fig. 4). However, the resting membrane potential (V_{rest}) decreased only slightly over time (Fig. 2a and Supplementary Fig. 3b). Notably, V_{rest} was significantly more negative than E_{GABA} during the first two weeks after viral injection (Fig. 2a). Thus, GABA initially depolarizes newborn DGCs in the adult brain.

The polarity of GABA action is largely determined by neuronal $[Cl^-]_i$ (refs 9–12). Sequential expression of the Na^+-K^+-$2Cl^-$ transporter NKCC1 (a Cl^- importer) and the K^+-coupled Cl^- transporter KCC2 (a Cl^- exporter) is believed to underlie the conversion from depolarization to hyperpolarization by GABA during neuronal maturation in the fetal brain[9–12]. We found that newborn DGCs (doublecortin-positive) in the adult brain express high levels of NKCC1 and little KCC2 (Fig. 2b and Supplementary Fig. 5b, c). We constructed several retroviruses expressing specific short hairpin RNAs (shRNA) against different regions of mouse *Nkcc1* (also known as *Slc12a2*) (ref. 22). We found that two different *Nkcc1*-shRNAs, but not the control shRNA, almost completely knocked down the expression of NKCC1 as shown by western blot analysis of HEK293 cells (Supplementary Fig. 5a) and immunostaining of newborn DGCs (Fig. 2b and Supplementary Fig. 5b). None of these shRNAs affected KCC2 expression in the infected cells *in vivo* (Fig. 2b and Supplementary Fig. 5c). GFP^+ DGCs expressing *Nkcc1*-shRNA, but not the control shRNA, had significantly lower $[Cl^-]_i$ (Supplementary Fig. 4). In addition, E_{GABA} was more negative than V_{rest} in the *Nkcc1*-shRNA-expressing DGCs throughout their development (Fig. 2c). Under perforated patch recording using gramicidin, tonic GABA activation led to hyperpolarization of *Nkcc1*-shRNA-expressing DGCs at 7 dpi, in contrast to depolarization of the control newborn DGCs (Fig. 2d). The amplitude of the tonic GABA currents under whole-cell recording, however, was similar (Fig. 2d), suggesting that the expression levels of functional $GABA_A$ receptors responsible for the tonic activation was not significantly affected.

We next examined the synaptic integration of new DGCs in the absence of GABA-induced depolarization *in vivo*. GABA-mediated

[1]Institute for Cell Engineering, Departments of Neurology and Neuroscience, Johns Hopkins University School of Medicine, Baltimore, Maryland 21205, USA.
*These authors contributed equally to this work.

synaptic transmission was examined in the presence of kynurenic acid (5 mM), which blocks ionotropic glutamate-mediated currents (Fig. 3a–c). We could not detect any PSCs in *Nkcc1*-shRNA-expressing DGCs at 7 dpi (Fig. 3a, b). The mean amplitude of the recorded PSCs at 14 and 28 dpi was only about 12% and 65% of those observed in control GFP^+ DGCs, respectively (Fig. 3b). In addition, the frequency of SSCs recorded at 28 dpi, but not the mean amplitude, was also significantly reduced (Fig. 3c), further indicating defects in the formation of GABA-mediated synapses by *Nkcc1*-shRNA-expressing cells.

We then examined glutamate-mediated synaptic transmission in the presence of bicuculline (10 μM) to block ionotropic GABA-mediated currents (Fig. 3d–f). We could not detect any PSCs or SSCs in *Nkcc1*-shRNA-expressing DGCs at 14 dpi, and the percentage of cells recorded with PSCs was greatly reduced at 28 dpi (Fig. 3d, e). Moreover, the mean peak amplitude of PSCs and frequency of SSCs at 28 dpi were only about 42% and 7% of those from control GFP^+ DGCs, respectively (Fig. 3e, f). The mean amplitude of SSCs, however, was not significantly different (Fig. 3f), suggesting that there were no general defects in receptor expression at the synapses.

We also examined the synaptic integration of newborn DGCs in *Nkcc1* germline knockout (*Nkcc1*$^{-/-}$) mice[23]. Despite the caveats of defects and potential compensation during embryonic development[11], we found similar defects in the formation of GABA- and glutamate-mediated synapses by newborn DGCs in adult *Nkcc1*$^{-/-}$ mice (Supplementary Fig. 6). Taken together, these results suggest that GABA-induced depolarization is essential for the establishment of functional GABA- and glutamate-mediated synapses for newly generated DGCs in the adult brain.

To directly examine the functional role of GABA-induced depolarization in the structural plasticity of newborn neurons, we used confocal microscopy to reconstruct the dendritic arborization of GFP^+ DGCs at 14 dpi (Fig. 4a), when active synaptogenesis occurs for GABA- and glutamate-mediated inputs. Consistent with results from the electrophysiological studies, we found that *Nkcc1*-shRNA-expressing DGCs had marked defects in dendritic arborization (Fig. 4b, c). The total dendritic length and branch number of these new neurons, as well as their dendritic complexity, were significantly reduced. In addition, we found that injection of the $GABA_A$ receptor agonist pentobarbital[20] seems to promote dendrite growth of newborn DGCs *in vivo* (Supplementary Fig. 7). Thus, GABA-induced depolarization/excitation regulates the dendritic development of newborn neurons in the adult brain.

Combining electrophysiology with retrovirus-mediated birth-dating and labelling, we have delineated the sequential steps involved in the integration of newly generated neurons into the pre-existing functional circuitry in the adult brain: from tonic GABA activation to GABA-mediated synaptic innervation and finally glutamate-mediated synaptic innervation (Figs 1, 3). GABA exerts a depolarizing action during the initial development of new DGCs due to their high $[Cl^-]_i$ from the expression of NKCC1 (Fig. 2). Using a retrovirus-mediated 'single-cell genetic' approach, we have shown that converting GABA-induced depolarization into hyperpolarization led

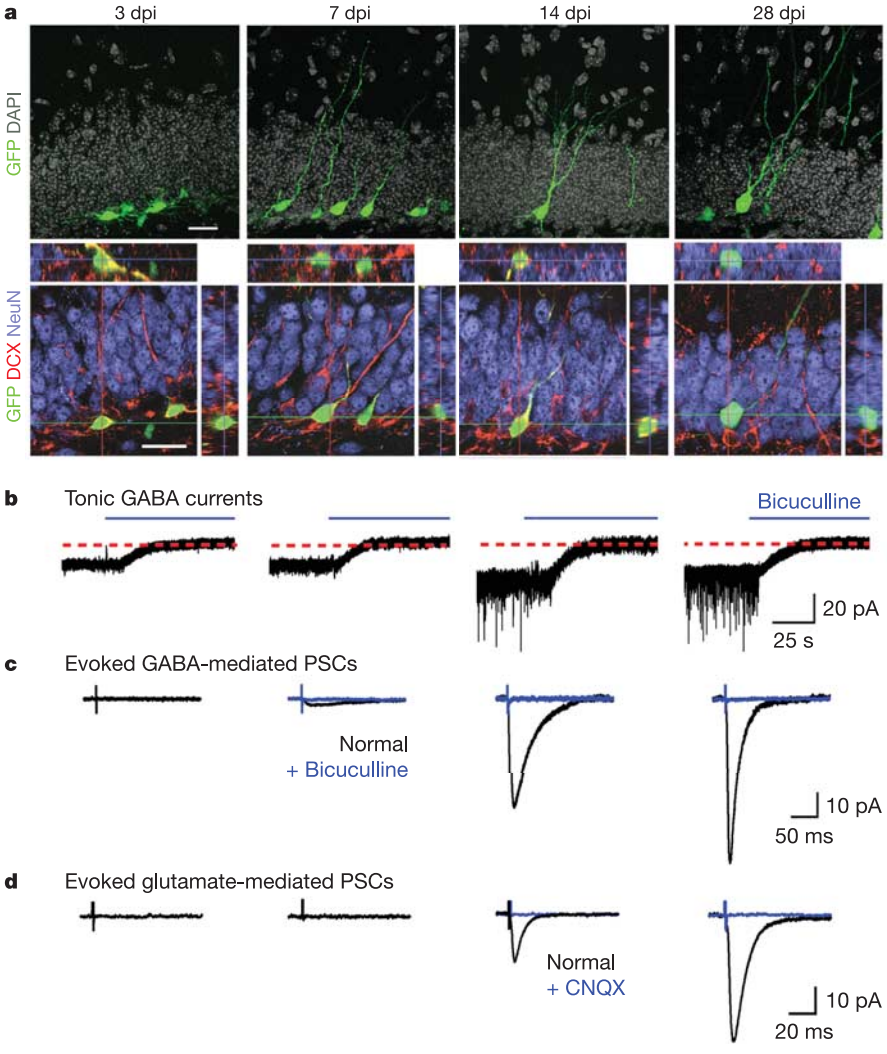

Figure 1 | Development of newborn DGCs in the adult mice. a, Confocal images of new DGCs (GFP^+, green) at different stages. Shown are projections (top) and confocal images of immunostaining (bottom) for doublecortin (DCX, red) and neuron-specific nuclear protein (NeuN, blue) with orthogonal views to confirm the co-localization of GFP and DCX or NeuN. Scale bars, 20 μm. **b–d**, Synaptic integration of newborn DGCs. Shown are sample recording traces from GFP^+ DGCs under whole-cell voltage-clamp ($V_m = -65$ mV). Tonic currents shown (**b**) are continuous recordings before and after adding bicuculline (100 μM, blue). Evoked PSCs shown are averaged responses from 5 consecutive stimuli before (black) and after (blue) adding bicuculline (10 μM, **c**) or CNQX (50 μM, **d**), respectively.

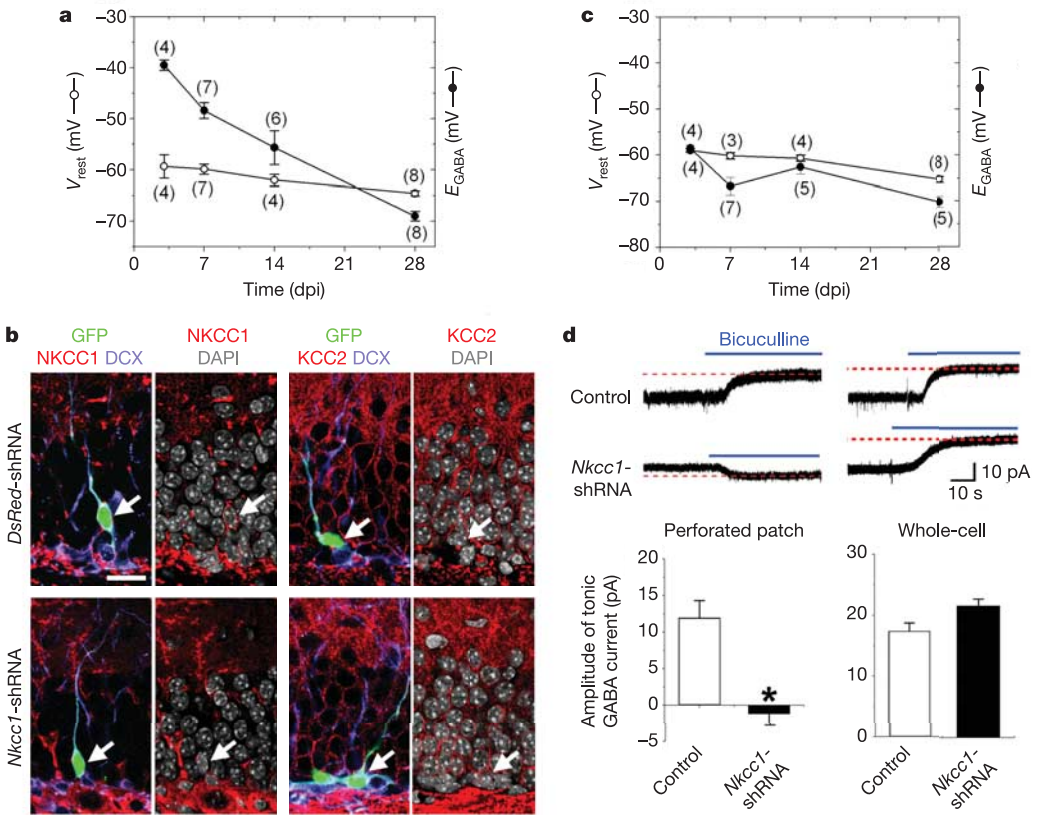

Figure 2 | Nature of GABA-induced activation in newborn DGCs in the adult brain. **a**, Resting membrane potentials (V_{rest}) and GABA-reversal potentials (E_{GABA}) of GFP$^+$ DGCs. Data show mean ± s.e.m. Numbers associated with symbols refer to the number of cells examined. **b**, Retrovirus-mediated co-expression of GFP and shRNAs specific for *Nkcc1*, but not a control shRNA (*DsRed*-shRNA), reduced NKCC1 expression but had no effects on KCC2 expression in newborn DGCs (7 dpi). Shown are confocal images of GFP (green) and immunostaining for NKCC1 or KCC2 (red), DCX (blue) and DAPI (grey). Arrows point to GFP$^+$ DGCs. Scale bar, 20 μm. **c**, V_{rest} and E_{GABA} in *Nkcc1*-shRNA-expressing newborn DGCs (similar to **a**). **d**, Tonic GABA currents in newborn DGCs (7 dpi) recorded under perforated patch (with gramicidin) or break-in whole-cell recording ($V_m = -65$ mV). Blue lines indicate the addition of bicuculline (100 μM). Values in bar graphs represent mean ± s.e.m. ($n = 6$, $^*P < 0.01$, ANOVA).

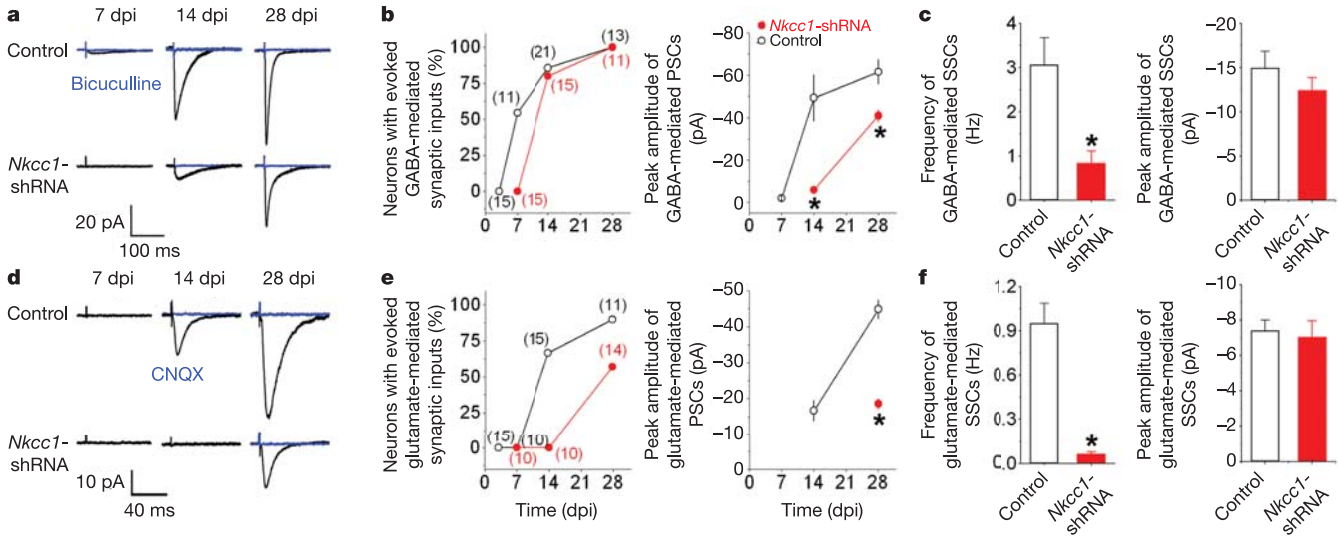

Figure 3 | Synaptic integration of newborn DGCs in the adult brain. **a–c**, Formation of GABA-mediated synaptic inputs by GFP$^+$ DGCs. Shown in **a** are sample traces of evoked PSCs recorded under whole-cell voltage-clamp ($V_m = -65$ mV, 5 mM kynurenic acid in the bath) before and after the addition of bicuculline (10 μM). **b**, **c**, The percentages of GFP$^+$ DGCs with detectable GABA-mediated PSCs, the mean peak amplitude of GABA-mediated PSCs (**b**), and mean frequency and peak amplitude of GABA-mediated SSCs recorded at 28 dpi (**c**). Numbers associated with symbols refer to the number of cells examined. Values represent mean ± s.e.m. ($^*P < 0.01$, ANOVA). **d–f**, Formation of glutamate-mediated synaptic inputs by GFP$^+$ DGCs. Same as **a–c**, except that the recordings were carried out in the presence of bicuculline (10 μM). Blue lines in **d** indicate the addition of CNQX (50 μM).

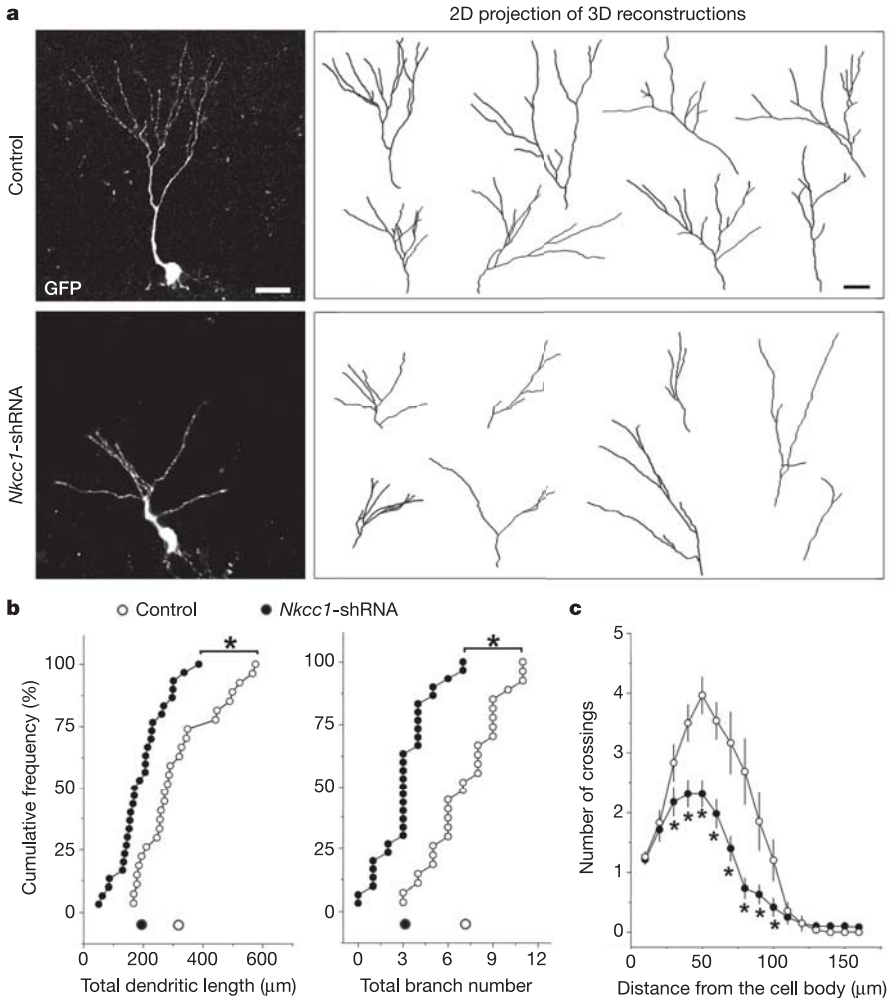

Figure 4 | Dendritic development of newborn DGCs in the adult brain. **a**, Confocal three-dimensional (3D) reconstruction of dendrites of control or *Nkcc1*-shRNA-expressing DGCs (14 dpi). Scale bar, 20 μm. **b**, Quantification of total dendritic length and branch number of newborn DGCs. Each symbol represents data from a single control (empty) or *Nkcc1*-shRNA-expressing (filled) DGC at 14 dpi. Symbols on the *x* axis represent mean values. (*$P < 0.01$, Kolmogorov–Smirnov test). **c**, Sholl analysis of dendritic complexity of GFP^+ DGCs (14 dpi). Values represent mean ± s.e.m. ($n = 27$; *$P < 0.05$, Student's *t*-test).

to significant defects in the formation of GABA- and glutamate-mediated synapses as well as in the dendritic development of newly generated neurons in the adult brain (Figs 3, 4). In the adult brain, ambient GABA is known to regulate the excitability of certain mature neurons, notably in the cerebellum and dentate gyrus[13–15,24,25]. Here we have shown that tonic GABA activation depolarizes newborn DGCs (Fig. 2 and Supplementary Fig. 3c), and more importantly, it constitutes the bulk of GABA-induced activation during the initial integration process when the phasic GABA activation either does not exist or is weaker than the tonic activation (Figs 2d and 3b, c). The mechanism by which tonic GABA activation regulates neuronal development and synaptic integration of new DGCs in the adult brain remains to be determined. Both voltage-dependent[8] and -independent Ca^{2+}-permeable channels[26] could be involved. Newborn DGCs in the adult brain express high levels of low-voltage activated T-type Ca^{2+} channels that are activated below −57 mV (ref. 8). Thus, tonic depolarization by GABA may lead to an activation of these Ca^{2+} channels and subsequent Ca^{2+} influx. Tonic activation may also provide an initial depolarization that allows a small phasic GABA activation to reach the threshold of these Ca^{2+} channels.

Activity-dependent anatomical reorganization is widely regarded as a fundamental mechanism of developmental and adult neural plasticity[27,28]. Within the dentate gyrus, principal neurons and interneurons form extensive recurrent connections. The levels of ambient GABA, regulated by interneuron activities (Supplementary Fig. 2c), may serve as a general indicator of dynamic neuronal network activity. Our study thus suggests an unexpected mechanism for activity-dependent regulation of adult neurogenesis, in which newborn neurons, before receiving any synaptic innervations, may sense neuronal network activities through local ambient GABA levels. Many physiological and pathological stimulations, including neurosteroids and epilepsy, affect GABA signalling[15,25] and might therefore influence the integration of new neurons in the adult brain. Our study might also have important implications for the use of stem cells in neuronal cell-replacement therapy for degenerative neurological diseases.

METHODS

See Supplementary Information for detailed methods.

Construction, production and stereotaxic injection of engineered retroviruses. Engineered self-inactivating murine retroviruses were used to label and genetically manipulate proliferating cells and their progeny[6,7]. GFP and shRNA were co-expressed under the control of the EF1α and human U6 promoters[22], respectively. The following short hairpin sequences were used: ACACACTTGTCCTGGGATT (*Nkcc1*-shRNA1); GGACAATATCTACCCAGCT (*Nkcc1*-shRNA2); AGTTCCAGTACGGCTCCAA (DsRed-shRNA). The specificity and efficiency of the shRNAs were validated, and high titres of engineered retroviruses (1×10^9 units ml^{-1}) were produced as previously described[6].

Adult (7–8-week-old) female C57BL/6 mice (Charles River) and *Nkcc1*$^{-/-}$ mice[23] housed under standard conditions were anaesthetized and retroviruses were stereotaxically injected at four sites (0.5 μl per site at 0.25 μl min^{-1}) with the following coordinates (from bregma in mm), as previously described[6]: anterioposterior, −2; lateral, ±1.6; ventral, 2.5; and anterioposterior, −3; lateral, ±2.6; ventral, 3.2. A total of 530 animals were used and all animal procedures were treated in accordance with institutional guidelines.

Immunostaining, confocal imaging and analysis. Coronal brain sections (40 μm thick) were prepared and processed for immunostaining using the following antibodies, as previously described[6]: goat anti-DCX (Santa Cruz; 1:500), mouse anti-NeuN (Chemicon; 1:200), mouse anti-NKCC1 (T4,

Developmental Studies Hybridoma Bank; 1:200), rabbit anti-KCC2 (Upstate; 1:200) and rabbit anti-Ki67 (Novocastra; 1:500). Sections were also stained for 4′,6-diaminodino-2-phenylindole (DAPI; 1:5,000). Images were acquired on a Zeiss LSM 510 META multiphoton confocal system using a multi-track configuration. For dendritic analysis, three-dimensional reconstructions of the dendritic processes of each GFP^+ neuron were made from *Z*-series stacks of confocal images. The projection images were semi-automatically traced with NIH ImageJ using the NeuronJ plugin. Total dendritic length and branch number of each individual GFP^+ neuron in the granule cell layer were analysed. Statistical significance ($P < 0.01$) was assessed using the Kolmogorov–Smirnov test. The Sholl analysis for dendritic complexity was carried out by counting the number of dendrites that cross a series of concentric circles at 5-μm intervals from the soma. Statistical significance ($P < 0.05$) was assessed using Student's *t*-test.

Electrophysiology. Mice housed under standard conditions were processed for slice preparation and electrophysiology as previously described[6]. Electrophysiological recordings were obtained at 32–34 °C. GFP^+ DGCs were identified by their green fluorescence, location within the subgranule or granule cell layer, neuronal morphology and capacity to generate Na^+ spikes (7 dpi and onwards). We monitored V_{rest} based on the reversal potential of the K^+ current through cell-attached patches (Supplementary Fig. 3b), to avoid underestimation of V_{rest} due to a shunt through the seal contact between the pipette and the membrane in perforated and whole-cell recording[18,29,30]. Microelectrodes (4–6 MΩ) were filled with the following solution: 120 mM potassium gluconate, 15 mM KCl, 4 mM $MgCl_2$, 0.1 mM EGTA, 10.0 mM HEPES, 4 mM MgATP, 0.3 mM Na_3GTP, 7 mM phosphocreatine (pH 7.4, 300 mOsm). For characterizing tonic GABA currents, potassium salt was substituted with CsCl in the intracellular solution and tetrodotoxin (0.5 μM) was added to the recording solution[14]. Additional drugs were used at following final concentrations: bicuculline (100 μM, Sigma), SR95531 (100 μM, Tocris), NO-711 (2.5 μM, Sigma).

Data were collected using an Axon 200B amplifier and acquired with a DigiData 1322A (Axon Instruments) at 10 kHz. Series and input resistances were monitored, and only those with changes less than 20% during experiments were analysed. The series resistance ranged from 10–30 MΩ and was uncompensated. For perforated patch recordings, the gramicidin stock (10 mg ml^{-1} in DMSO) was diluted in the pipette solution (135 mM CsCl, 4 mM $MgCl_2$, 0.1 mM EGTA, 10 mM HEPES, pH 7.4, 300 mOsm) to a final concentration of 25 μg ml^{-1} just before experiments. Perforated patch recordings with a series resistance of <80 MΩ and without significant changes (>25%) during recordings were used for data analysis.

For measurement of E_{GABA}, focal pressure ejection of 10 μM GABA through a puffer pipette controlled by a Picrospitzer (5-ms puff at 3–5 psi) was used to activate $GABA_A$ receptors on the GFP^+ DGCs with gramicidin perforated patch under voltage-clamp at different holding potentials (Supplementary Fig. 3a). The peak amplitude and holding potential were plotted and E_{GABA} was determined for each cell. Intracellular chloride concentrations were calculated using the following equation: $[Cl^-]_i = [Cl^-]_o e(E_{GABA}F/RT)$, where the extracellular Cl^- concentration $[Cl^-]_o$ is 134.1 mM (Supplementary Fig. 4).

A bipolar electrode (World Precision Instruments) was used to stimulate (100-μs duration) the perforant pathway input to the dentate gyrus. The stimulus intensity (~30 μA) was maintained for all experiments. To examine the evoked synaptic transmission, a train of 20 stimuli was delivered at 0.1 Hz. To confirm a lack of evoked synaptic transmission, the stimulation intensity was then increased to 200 μA.

Received 1 September; accepted 8 November 2005.
Published online 11 December 2005.

1. Kempermann, G. & Gage, F. H. New nerve cells for the adult brain. *Sci. Am.* **280,** 48–53 (1999).
2. Fuchs, E. & Gould, E. Mini-review: *in vivo* neurogenesis in the adult brain: regulation and functional implications. *Eur. J. Neurosci.* **12,** 2211–2214 (2000).
3. Temple, S. & Alvarez-Buylla, A. Stem cells in the adult mammalian central nervous system. *Curr. Opin. Neurobiol.* **9,** 135–141 (1999).
4. Doetsch, F. & Hen, R. Young and excitable: the function of new neurons in the adult mammalian brain. *Curr. Opin. Neurobiol.* **15,** 121–128 (2005).
5. Ming, G.-l. & Song, H. Adult neurogenesis in the mammalian central nervous system. *Annu. Rev. Neurosci.* **28,** 223–250 (2005).
6. van Praag, H. *et al.* Functional neurogenesis in the adult hippocampus. *Nature* **415,** 1030–1034 (2002).
7. Carleton, A., Petreanu, L. T., Lansford, R., Alvarez-Buylla, A. & Lledo, P. M. Becoming a new neuron in the adult olfactory bulb. *Nature Neurosci.* **6,** 507–518 (2003).
8. Schmidt-Hieber, C., Jonas, P. & Bischofberger, J. Enhanced synaptic plasticity in newly generated granule cells of the adult hippocampus. *Nature* **429,** 184–187 (2004).
9. Ben-Ari, Y. Excitatory actions of GABA during development: the nature of the nurture. *Nature Rev. Neurosci.* **3,** 728–739 (2002).
10. Owens, D. F. & Kriegstein, A. R. Is there more to GABA than synaptic inhibition? *Nature Rev. Neurosci.* **3,** 715–727 (2002).
11. Delpire, E. Cation-chloride cotransporters in neuronal communication. *News Physiol. Sci.* **15,** 309–312 (2000).
12. Payne, J. A., Rivera, C., Voipio, J. & Kaila, K. Cation-chloride co-transporters in neuronal communication, development and trauma. *Trends Neurosci.* **26,** 199–206 (2003).
13. Overstreet, L. S. & Westbrook, G. L. Paradoxical reduction of synaptic inhibition by vigabatrin. *J. Neurophysiol.* **86,** 596–603 (2001).
14. Nusser, Z. & Mody, I. Selective modulation of tonic and phasic inhibitions in dentate gyrus granule cells. *J. Neurophysiol.* **87,** 2624–2628 (2002).
15. Farrant, M. & Nusser, Z. Variations on an inhibitory theme: phasic and tonic activation of $GABA_A$ receptors. *Nature Rev. Neurosci.* **6,** 215–229 (2005).
16. Wang, L. P., Kempermann, G. & Kettenmann, H. A subpopulation of precursor cells in the mouse dentate gyrus receives synaptic GABAergic input. *Mol. Cell. Neurosci.* **29,** 181–189 (2005).
17. Wadiche, L. O., Bromberg, D. A., Bensen, A. L. & Westbrook, G. L. GABAergic signalling to newborn neurons in dentate gyrus. *J. Neurophysiol.* **94,** 4528–4532 (2005).
18. Wang, D. D., Krueger, D. D. & Bordey, A. GABA depolarizes neuronal progenitors of the postnatal subventricular zone via $GABA_A$ receptor activation. *J. Physiol. (Lond.)* **550,** 785–800 (2003).
19. Liu, X., Wang, Q., Haydar, T. F. & Bordey, A. Nonsynaptic GABA signalling in postnatal subventricular zone controls proliferation of GFAP-expressing progenitors. *Nature Neurosci.* **8,** 1179–1187 (2005).
20. Tozuka, Y., Fukuda, S., Namba, T., Seki, T. & Hisatsune, T. GABAergic excitation promotes neuronal differentiation in adult hippocampal progenitor cells. *Neuron* **47,** 803–815 (2005).
21. Owens, D. F., Boyce, L. H., Davis, M. B. & Kriegstein, A. R. Excitatory GABA responses in embryonic and neonatal cortical slices demonstrated by gramicidin perforated-patch recordings and calcium imaging. *J. Neurosci.* **16,** 6414–6423 (1996).
22. Paddison, P. J., Caudy, A. A., Bernstein, E., Hannon, G. J. & Conklin, D. S. Short hairpin RNAs (shRNAs) induce sequence-specific silencing in mammalian cells. *Genes Dev.* **16,** 948–958 (2002).
23. Delpire, E., Lu, J., England, R., Dull, C. & Thorne, T. Deafness and imbalance associated with inactivation of the secretory Na-K-2Cl co-transporter. *Nature Genet.* **22,** 192–195 (1999).
24. Chadderton, P., Margrie, T. W. & Hausser, M. Integration of quanta in cerebellar granule cells during sensory processing. *Nature* **428,** 856–860 (2004).
25. Semyanov, A., Walker, M. C., Kullmann, D. M. & Silver, R. A. Tonically active $GABA_A$ receptors: modulating gain and maintaining the tone. *Trends Neurosci.* **27,** 262–269 (2004).
26. Chavas, J., Forero, M. E., Collin, T., Llano, I. & Marty, A. Osmotic tension as a possible link between $GABA_A$ receptor activation and intracellular calcium elevation. *Neuron* **44,** 701–713 (2004).
27. Cline, H. T. Dendritic arbor development and synaptogenesis. *Curr. Opin. Neurobiol.* **11,** 118–126 (2001).
28. Wong, R. O. & Ghosh, A. Activity-dependent regulation of dendritic growth and patterning. *Nature Rev. Neurosci.* **3,** 803–812 (2002).
29. Tyzio, R. *et al.* Membrane potential of CA3 hippocampal pyramidal cells during postnatal development. *J. Neurophysiol.* **90,** 2964–2972 (2003).
30. Verheugen, J. A., Fricker, D. & Miles, R. Noninvasive measurements of the membrane potential and GABAergic action in hippocampal interneurons. *J. Neurosci.* **19,** 2546–2555 (1999).

Supplementary Information is linked to the online version of the paper at www.nature.com/nature.

Acknowledgements We would like to thank C. F. Stevens, F. H. Gage, R. Huganir, K.-W. Yau and J. Bischofberger for comments and suggestions, L-h. Liu for technical support, E. Delpire for *Nkcc1* knockout mice and mouse *Nkcc1* cDNA, and N. Gaiano, D. Sun, D. K. Ma and D. Pradhan for reagents and help. This work was supported by the National Institute of Health (H.S.), Klingenstein Fellowship Awards in the Neurosciences (G-l.M. and H.S.), the Whitehall Foundation (G-l.M.) and The Robert Packard Center for ALS Research at Johns Hopkins (H.S.).

Author Contributions S.G. did virus injection and electrophysiology, E.L.K.G. engineered retroviral constructs and did characterization, K.A.S. did immunohistochemistry and confocal imaging analysis, and Y.K. helped with molecular biology. G-l.M. and H.S. are senior authors and were responsible for project planning. All authors discussed the results and commented on the manuscript.

Author Information Reprints and permissions information is available at npg.nature.com/reprintsandpermissions. The authors declare no competing financial interests. Correspondence and requests for materials should be addressed to H.S. (shongju1@bs.jhmi.edu) or G-l.M. (gming1@bs.jhmi.edu).